Effect of Design Parameter Variation on Flat Plate Solar Collector Efficiency Using Nano Working Fluids

Talib Onimisi Ahmadu*‡, Muideen Bolarinwa Balogun*, Hamisu Adamu Dandajeh*

*Department of Mechanical Engineering, Faculty of Engineering, Ahmadu Bello University, Zaria, Nigeria.

(talibahmadu@gmail.com, balo.muyi@gmail.com, hadandajeh@yahoo.com)

‡Corresponding author: Talib Onimisi Ahmadu, Department of Mechanical Engineering, Faculty of Engineering, Ahmadu Bello University, Zaria, Nigeria,

Tel: +234 – 8023824226, talibahmadu@gmail.com

Received: 09.03.2022 Accepted: 21.04.2022

Abstract- Water, which is the most commonly used working fluid limits the efficiency of flat plate solar collectors due to its poor heat transfer properties. Also, proper sizing of collector design parameters is a major factor for enhanced efficiency. In this study, the efficiency of a flat plate solar collector was simulated using water and three different nano working fluids: graphene, aluminium oxide and copper oxide nano fluids. Three different mass fractions of nano particles: 0.025, 0.05 and 0.075 weight percent (wt. %) were used for each of the nano fluids. Collector performance equations were programmed and simulated in MATLAB, using collector area of 1.2 m^2, average solar radiation of 750 W/m^2 and inlet working fluid temperature of 40°C. The collector design parameters: tube spacing, fluid mass flow rate, and tube diameter were varied and the effect on efficiency determined. Results indicated that efficiency increased with increase in mass fraction for all the nano working fluids. Increasing the tube spacing increased the efficiency to a maximum, from where it then decreased. Also, increase in mass flow rate resulted in increase in efficiency to a maximum, from where efficiency then remained constant. While there was very marginal increase in efficiency with increase in tube diameter for all the working fluids. For graphene, aluminium oxide, copper oxide and water working fluids respectively, tube spacing between 0.1 to 0.12 m produced highest efficiencies of 0.78, 0.7, 0.63 and 0.53. Mass flow rate of 0.1 kg/s gave maximum efficiencies of 0.78, 0.7, 0.68 and 0.53. At zero loss efficiency point and mass fraction of 0.075 wt. %, increase in collector efficiency attained by the nano fluids over water as working fluid were 28%, 22.8% and 19.2% for graphene, aluminium oxide and copper oxide nano fluids respectively.

Keywords Nano working fluid, collector, efficiency, simulation, MATLAB

1. Introduction

The continuous decrease in the reserves of conventional fuel resources on the earth has led to increased research interest in renewable sources of energy, such as solar energy [1]. Solar energy stands out from other available renewable energy sources due to its availability and environmentally friendly nature [2]. The major component of solar water heating system is the solar collector. This captures the incoming solar radiation, then converts it to thermal energy of a working fluid flowing through the collector tubes. It is this thermal energy in the working fluid that is then transferred to the desired application [2].

Flat plate solar collectors are most widely used for applications that require low to medium fluid temperature. They are simple in design and construction, as well as low in cost and maintenance. However, they have relatively low efficiencies when compared to other types of collectors [3]. Several solar thermal systems, including solar thermal desalination also make use of flat plate collectors [4]. Hence the need for improved flat plate collector design for enhanced efficiency [5]. Conventional working fluids used in flat plate collectors include water, ethylene glycol, oils. These fluids have poor heat transfer properties which limit the heat transfer to the fluids and thereby cause a reduction in efficiency of the collector [1]. Also, proper sizing of flat plate collector design parameters such as tube spacing, tube

diameter, tube length, mass flow rate have significant effect on the collector efficiency.

Several researchers have employed experimental and numerical studies to investigate the prospects of utilizing nanofluids and other non-conventional working fluids to improve flat plate collector efficiency. Reference [6], studied the effect of using propylene glycol – water as working fluid in flat plate collector. They concluded that increasing the propylene glycol volume concentration from 25% to 50% increases the efficiency of the collector. Reference [7], carried out the evaluation of the heat transfer performance of a flat plate solar collector using TiO_2/ water and CuO/ water nanofluids as working fluids. They reported a maximum efficiency of 55%, 54% and 50% for the CuO/water, TiO_2/ water and water respectively for 0.1% concentration by volume of the nanofluids. Reference [8], studied the performance of a solar water heater by incorporating a transparent nanomaterial; fluorine doped tin oxide to the collector. They concluded that the nano material improved the system efficiency. Reference [9], studied the effect of clove treated graphene nanoplatelet nanofluid on the performance of flat plate solar collector. They concluded that solar collector thermal performance increased with an increase in mass concentration of graphene. Reference [10] experimentally evaluated the performance of a solar collector using Al_2O_3 nanofluid as working fluid. They concluded that the Al_2O_3 nonofluid with 0.1, 0.3 and 0.5 weight concentration improved the collector fluid outlet temperature by 0.4%, 8.1% and 11.6% respectively compared to that of distilled water. Reference [11], experimentally investigated the performance of flat plate solar collector using graphene – water nanofluid of varying mass concentration. Maximum increase in efficiency of 13% over water was recorded. Reference [12] conducted experimental study of Cu – water nano fluid as working fluid in flat plate solar collector. Results indicate that at 0.05 weight %, collector efficiency was increased by about 24% over water as working fluid. Reference [13] investigated flat plate collector performance using graphene nanoplatelets with distilled water as base fluid. Results indicated an increase in collector efficiency by 24.9% at 0.1% by weight. Also, they reported that colloidal instability and sedimentation, resulting in decreased concentration results after prolonged use of the nano fluid. Reference [14] developed an improved computer model for enhanced system performance. Reference [15] investigated the effect of graphene nanofluid on thermal performance of flat plate solar collectors, with water as base fluid. Results showed that graphene nanofluid of 0.025% by weight increased the thermal efficiency by 18.87% over the base fluid.

While studies on efficiency of flat plate solar collectors using nano working fluids are available in literature, studies on the effect of varying flat plate collector design parameters on the efficiency using nano working fluids are scarce. Proper sizing of collector design parameters has significant effect on efficiency. The present study intends to study, by way of simulation, the effect of varying tube spacing, tube diameter, and mass flow rate on flat plate collector efficiency using water, graphene, aluminium oxide and copper oxide nano working fluids.

2. Methodology

This section presents the methods employed in carrying out the present study.

2.1. The Nano Working Fluids

Nano fluids are fluids made of (1 – 100 nm) nano particles, suspended in different base liquids such as distilled water, ethylene glycol. The resulting nano fluids usually have enhanced thermal conductivity [11]. Three different nano fluids were used in the simulation in this study. They were obtained from three different nano particles: mono layer graphene, aluminium oxide and copper oxide. Water was taken as the base fluid for each of the nano particles. Three mass fractions of each of the nano particles in the base fluid were used: 0.025, 0.05 and 0.075 weight percent (wt. %). Table 1 shows the properties of the nano particles and base fluid (water) used in the simulation.

Table 1. Properties of nano particles

Material	Thermal conductivity (W/mK)	Specific heat capacity (J/kgK)	Density (kg/m^3)
Water	0.576	4180	1000
Graphene	2000	1.9	2000
$Al2O_3$	40	775	3970
CuO_2	32.9	525	6500

Source: (References [7], [16] and [17])

2.2. The software (MATLAB)

MATLAB, which is the short form for matrix laboratory is a high performance language for technical computing. It operates primarily on arrays and matrices. It is suitable for modelling, simulation and prototyping.

2.3. Collector Performance Modelling Equations

Equations that describe the performance and efficiency of flat plate solar collectors were programmed and simulated using MATLAB. The properties of the nano working fluids: density, specific heat capacity, thermal conductivity and viscosity were computed using the relations from literature. The following assumptions were made in the performance modelling:

i. Steady state conditions
ii. Constant wall temperature in the tubes
iii. Flow of fluid is in the fully developed regime
iv. Nano fluids act in single phase with good stability

The density of the nano fluids was computed according to reference [18] as:

$$\rho_{nf} = \omega\rho_{np} + (1-\omega)\rho_{bf} \quad (1)$$

The specific heat capacity of the nano fluids was computed according to reference [18] as:

$$C_{p,nf} = \omega C_{p,np} + (1-\omega)C_{p,bf} \quad (2)$$

The thermal conductivity of the nano fluids was computed according to reference [19] as:

$$k_{nf} = \frac{k_{np}+2k_{bf}+(k_{np}-k_{bf})\omega}{k_{np}+2k_{bf}-(k_{np}-k_{bf})\omega} k_{bf} \quad (3)$$

The viscosity was computed using the relation of [20] as:

$$\mu_{nf} = \mu_{bf}\left(1-\frac{\omega}{\varphi_m}\right)^{-2} \quad (4)$$

Where φ_m is the maximum packing fraction that the nanoparticles can achieve, given as:

$$\varphi_m = 5\times10^{-6}T_i^2 - 4\times10^{-4}T_i + 0.118 \quad (5)$$

The relations of reference [21], as given in equations 6 to 8 and 12 to 28 were used to compute the collector performance parameters:

The standard fin efficiency (F) was calculated using equation 6

$$F = \frac{\tanh\left(\frac{m(W-D_o)}{2}\right)}{\frac{m(W-D_o)}{2}} \quad (6)$$

Where m is given as:

$$m = \sqrt{\frac{U_L}{k_b\delta}} \quad (7)$$

The collector efficiency factor (F') was calculated according to equation 8

$$F' = \frac{\frac{1}{U_L}}{W\left[\frac{1}{U_L(D_o+(W-D_o)F)}+\frac{1}{C_b}+\frac{1}{\pi D_i h_{fi}}\right]} \quad (8)$$

Where; equations 9 to 11 were evaluated according to reference [22] as:

$$h_{fi} = \frac{k_{nf}}{D_i} 0.023Re\times0.8Pr^4 \quad (9)$$

$$Re = \frac{\rho_{nf}vD_i}{\mu_{nf}} \quad (10)$$

$$Pr = \frac{\mu_{nf}C_{p,nf}}{k_{nf}} \quad (11)$$

Also, from equation (8); $U_L = U_t + U_b + U_e$ (12)

U_L is the overall loss coefficient, U_t, U_b and U_e are the top, back and edge loss coefficients respectively, evaluated as follows:

$$U_t = \left[\frac{N}{\frac{c}{T_{pm}}\left[\frac{(T_{pm}-T_{amb})}{(N+f)}\right]^e}+\frac{1}{h_w}\right]^{-1} + \frac{\sigma(T_{pm}+T_{amb})(T_{pm}^2+T_{amb}^2)}{\frac{1}{\varepsilon_p+0.00591Nh_w}+\frac{2N+f-1+0.133\varepsilon_p}{\varepsilon_g}-N} \quad (13)$$

$$U_b = \frac{k_i}{l_i} \quad (14)$$

$$U_e = \frac{k_e}{x_e}\left[\frac{2(L+B)H}{LB}\right] \quad (15)$$

Where; $c = 520(1-0.000051\beta^2)$, for $0^o \ll \beta \ll 70^o$ (16)

$$e = 0.430\left(1-\frac{100}{T_{pm}}\right) \quad (17)$$

$$h_w = 5.7+3.8v \quad (18)$$

The heat removal factor (F_R) was calculated using equation 19

$$F_R = \frac{\dot{m}C_{p,nf}}{A_cU_L}\left[1-exp\left(-\frac{A_cU_LF'}{\dot{m}C_{p,nf}}\right)\right] \quad (19)$$

The useful energy gain by the collector (Q_u) was calculated using equations 20 to 22

$$Q_u = \dot{m}C_{p,nf}(T_o-T_i) \quad (20)$$

$$Q_u = \rho_{nf}\dot{Q}C_{p,nf}(T_o-T_i) \quad (21)$$

$$Q_u = A_cF_R[G(\tau\alpha)-U_L(T_i-T_a)] \quad (22)$$

The mean plate temperature was computed according to equation 23

$$T_{pm} = T_i + \frac{Q_u/A_c}{F_RU_L}(1-F_R) \quad (23)$$

The outlet fluid temperature (T_o) was computed according to equation 24

$$T_o = T_i + \left(\frac{Q_u}{\dot{m}C_{p,nf}}\right) \quad (24)$$

The efficiency of the flat plate collector (η) was computed using equations 25 to 28:

$$\eta = \frac{Q_u}{A_cG} \quad (25)$$

$$\eta = \frac{\dot{m}c_{p,nf}(T_o-T_i)}{A_cG} \quad (26)$$

$$\eta = \frac{A_cF_R[G(\tau\alpha)-U_L(T_i-T_a)]}{A_cG} \quad (27)$$

$$\eta = F_R(\tau\alpha) - F_RU_L\left(\frac{T_i-T_a}{G}\right) = \frac{\dot{m}C_p(T_o-T_i)}{A_cG_T} \quad (28)$$

2.4. Simulation Procedure

Equations 1 to 28 were programmed in MATLAB and used for the simulation. Properties of each of the nano working fluids were computed using equations 1 to 5, for mass fractions of 0.025, 0.05 and 0.075 wt. %. These properties were then used to compute the collector performance parameters using equations 6 to 28. When computing performance parameters for water as working fluid, properties of water were used in equations 6 to 28. Collector area of 1.2 m^2 was used, while inlet working fluid temperature of 40ºC was used. Average solar radiation of 750 W/m^2 and average ambient temperature of 27ºC were used. These were based on values obtained from simulation of monthly average solar radiation and ambient temperature in the summer months using the weather data of Zaria – Nigeria in the TRNSYS 16 software.

While computing the performance equations, an iterative procedure was employed. An initial mean plate temperature T_{pm}= 90ºC was used to calculate U_t, from which approximate values of F', F_R and Q_u were obtained. Equation 23 was then used to calculate new value of T_{pm}, resulting in new values of F', F_R and Q_u and the process continues.

The collector design parameters: fluid mass flow rate, tube spacing and tube diameter were varied for each mass fraction for each of the nano working fluids. These design parameters were also varied for water as working fluid. The fluid mass flow rate was varied from 0 to 0.5 kg/s, the tube spacing was varied from 0 to 1 m, while the tube diameter was varied from 0.01 to 0.05 m. The effects of varying the design parameters on the collector efficiency were studied. Values of design parameters that produced maximum efficiencies were then used to simulate collector performance, where equation 28 was used to simulate the variation of efficiency with reduced temperature parameter $\left(\frac{T_i-T_a}{G}\right)$. Details of the

collector design parameters used in the simulation are shown in table 2. Fig. 1 shows a flow chart of the simulation process in MATLAB.

Table 2. Collector design parameters

S/N	Parameter	Value
1	Collector area (m^2)	1.2
2	No. of glazing	1
3	Thickness of glazing (m)	0.005
4	Absorber plate thickness (m)	0.003
5	Plate emittance	0.95
6	Glass emittance	0.9
7	Transmittance absorptace product	0.79
8	Back insulation thickness (m)	0.07
9	Edge insulation thickness (m)	0.03
10	Tube length (m)	0.9
11	Tube diameter (m)	Varied (0.01 - 0.05)
12	Tube spacing (m)	Varied (0 - 1)
13	Mass flow rate (kg/s)	Varied (0 - 0.5)

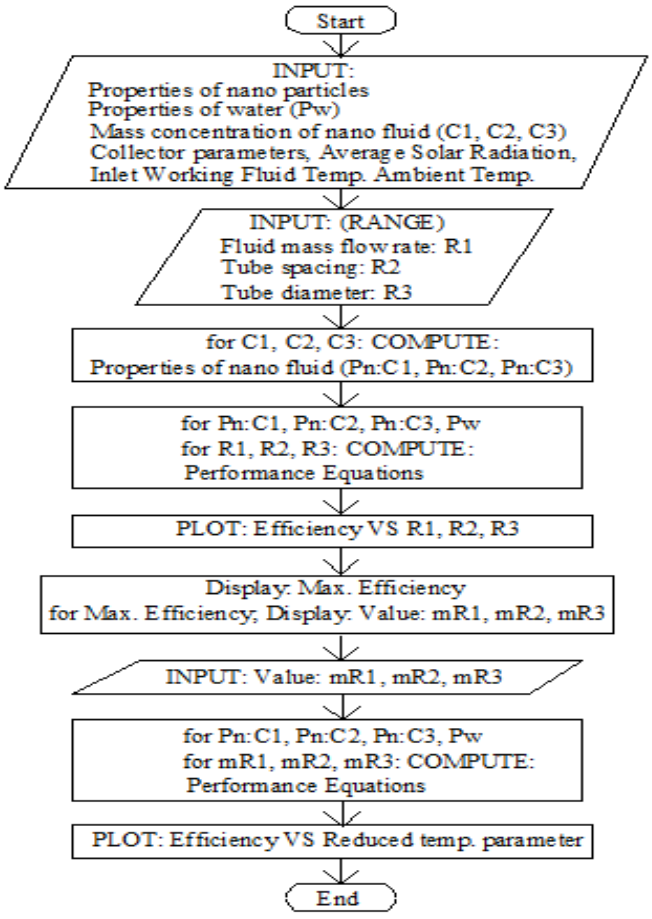

Fig. 1. Flow chart of simulation process in MATLAB

2.4. Validation of Simulation Model

The simulation model was validated using the work of reference [13]. Design parameter values and properties of graphene nanofluid used in the work of reference [13] were used in the model simulation. Results obtained were compared with experimental values obtained from the work. Fig. 2 shows the comparison of simulation and experimental values for the variation of efficiency with reduced temperature parameter, for graphene of mass fraction 0.025, 0.05 and 0.1 wt. %, as well as water. Lines of best fit were drawn through the points and extended to intersect at the efficiency axis, which show the zero loss efficiency points. Maximum deviation of simulated values from experimental results were found to be 3.8%, which shows good agreement between the two values, thus validating the model.

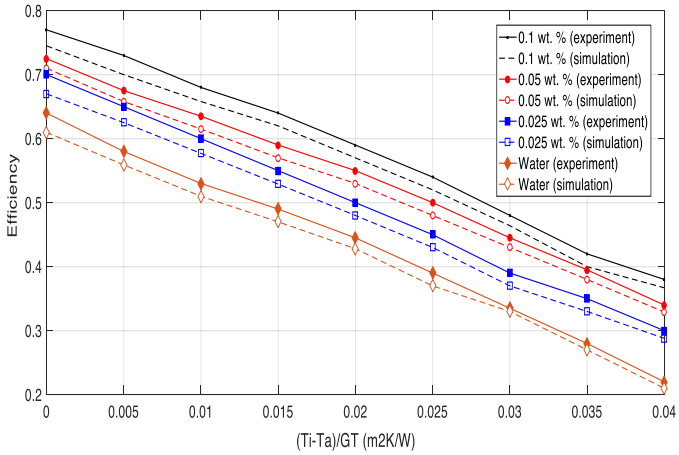

Fig. 2. Variation of efficiency with reduced temperature parameter (experiment/ simulation)

3. Results and Discussion

Figs. 3 (a) to 3 (c) show the variation of efficiency with tube spacing for all the working fluids at mass fractions of 0.025, 0.05 and 0.075 wt. % respectively. From the figures it can be observed that for all the working fluids, efficiency increases with increasing tube spacing up to an optimum value, from which it starts to decrease with increasing tube spacing. This is because increasing the tube spacing leads to reduction in number of tubes, which leads to lower volume of working fluid in the collector at a given instant. As the volume of working fluid continues to decrease after the optimum point, heat removal factor decreases and therefore efficiency decreases. The efficiency can be seen to increase with increase in mass fraction of nano particles for each of the nano working fluids. This is because increasing the mass fraction of the nano particles increases the thermal conductivity of the nano fluid. This leads to enhanced convective heat transfer, resulting in increased efficiency.

While water working fluid had constant efficiency of 0.53, efficiencies of the nano working fluids can be seen to be between 0.6 to 0.67, 0.62 to 0.71 and 0.63 to 0.78 for mass fractions of 0.025, 0.05 and 0.075 wt. % respectively. Graphene nano working fluid is seen to have produced the highest efficiency for each of the three mass fractions, while copper oxide nano working fluid produced the lowest efficiencies. Tube spacing of between 0.1 m to 0.12 m can be seen to have produced the highest efficiencies. The highest efficiency of 0.78 was obtained with graphene nano working

fluid at a mass fraction of 0.075 wt. % and tube spacing of 0.1 m. Aluminium oxide nano working fluid attained maximum efficiency of 0.7 at mass fraction of 0.075 wt. % and tube spacing of 0.1 m. Copper oxide nano working fluid attained maximum efficiency of 0.63 at 0.075 wt. % and tube spacing of 0.12 m.

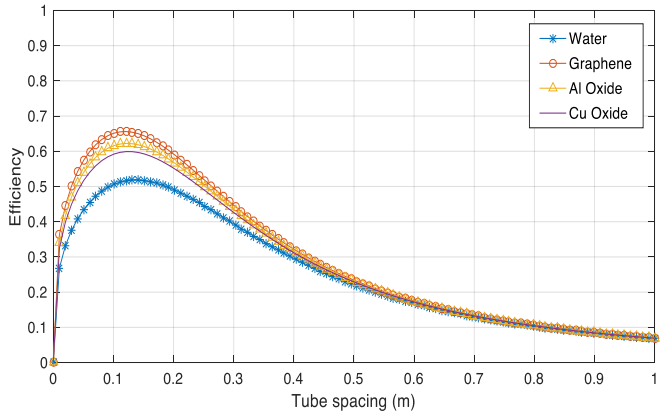

(a) Variation of efficiency with tube spacing (0.025 wt. %)

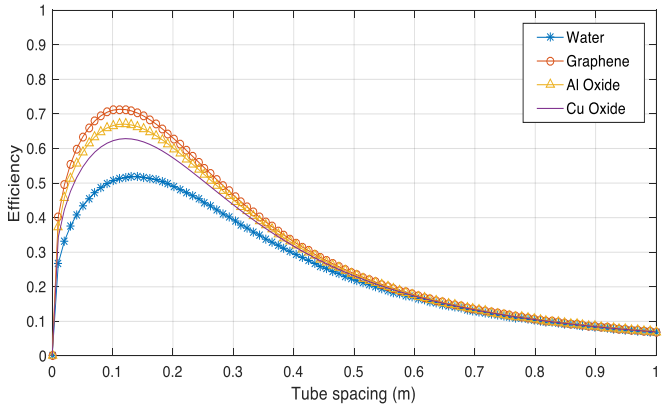

(b) Variation of efficiency with tube spacing (0.05 wt. %)

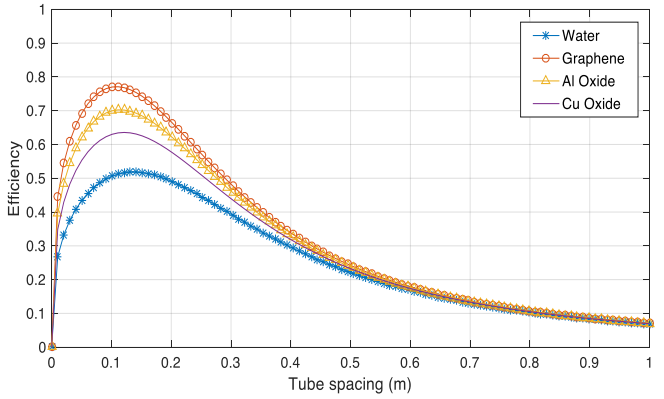

(c) Variation of efficiency with tube spacing (0.075 wt. %)

Fig. 3. Variation of efficiency with tube spacing

Figs. 4 (a) to 4 (c) show the variation of efficiency with mass flow rate for all the working fluids at mass fractions of nano particles of 0.025, 0.05 and 0.075 wt. % respectively. It can be observed from the figures that for all the working fluids, efficiency increases with increasing mass flow rate. However, for all the nano working fluids an optimum mass flow rate is attained, after which efficiency remains constant with increasing mass flow rate. This is because increasing mass flow rate results in increase in heat removal factor which translates to increase in efficiency. However, as the rate at which fluid flow through the collector continues to increase, it gets to a point where a portion of the fluid only flows through the collector and doesn't partake in heat transfer, and therefore doesn't contribute to increasing the heat removal factor. This leads to insignificant increase in efficiency or the efficiency remains constant after this point. An optimum mass flow rate of 0.1 kg/s is observed for all the nano working fluids.

From the figs. 4 (a) to 4 (c), efficiencies can be seen to increase with increasing mass fraction of nano particles. This is attributed to the enhanced convective heat transfer resulting from increase in mass fraction of nano particles. Efficiencies of 0.58 to 0.63, 0.61 to 0.7 and 0.68 to 0.78 are observed for mass fraction of nano particles of 0.025, 0.05 and 0.075 wt. % respectively. Maximum efficiencies of 0.78, 0.7 and 0.68 were observed for graphene, aluminium oxide and copper oxide nano working fluids respectively at 0.075 wt. %. Water showed a maximum efficiency of 0.53.

(a) Variation of efficiency with mass flow rate (0.025 wt. %)

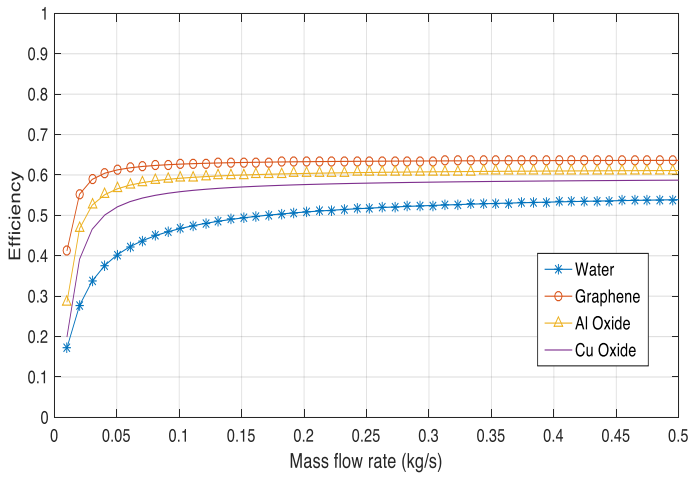

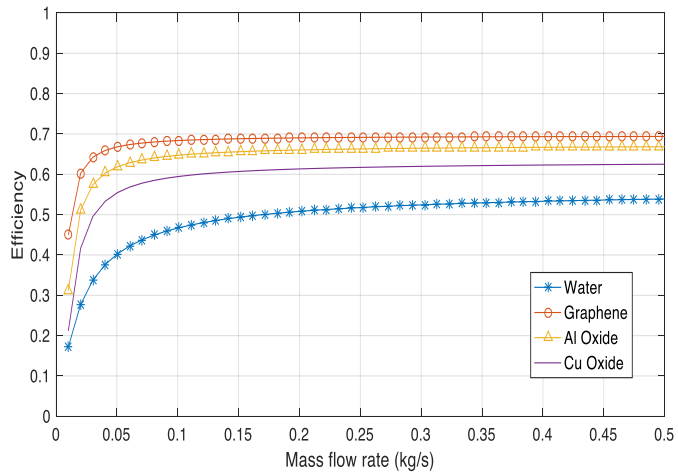

(b) Variation of efficiency with mass flow rate (0.05 wt. %)

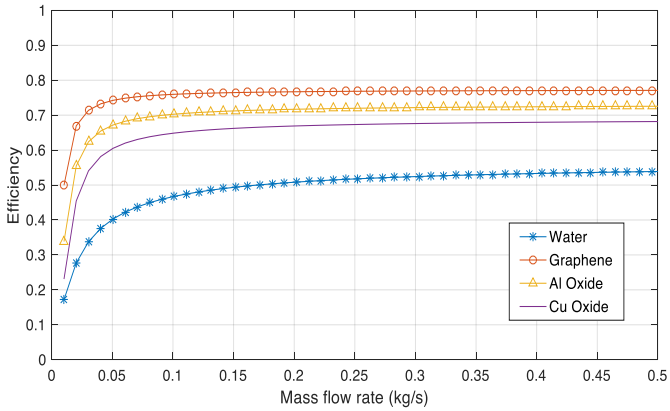

(c) Variation of efficiency with mass flow rate (0.075 wt. %)

Fig. 4. Variation of efficiency with mass flow rate

Figs. 5 (a) to 5 (c) show the variation of efficiency with tube diameter for all the working fluids at mass fractions of nano particles of 0.025, 0.05 and 0.075 wt. % respectively. As observed from the figures, for water as working fluid, there is no significant increase in efficiency as the tube diameter increases. For the nano working fluids, the increase in efficiency is very marginal as the tube diameter increases from 0.01 m to 0.05 m, for the three mass fractions of nano particles. This is because, irrespective of the tube diameter, mass flow rate is unchanged and thereby volume content of working fluid in the collector at a given time remains the same. This leads to unchanged efficiency or very marginal increase in efficiency which could be due to increase in heat transfer area of the tube.

Also, from the figs. 5 (a) to 5 (c), it is observed that efficiencies increase with increasing mass fraction of nano particles. This is as a result of increased convective heat transfer as nano particles increases. Efficiencies of 0.57 to 0.65, 0.62 to 0.7 and 0.64 to 0.75 were attained by the nano working fluids for mass fractions of 0.025, 0.05 and 0.075 wt. % respectively at 0.1 m tube diameter. Efficiencies of 0.75, 0.7 and 0.64 were attained by graphene, aluminium oxide and copper oxide nano working fluids respectively, at 0.075 wt. % and 0.1 m tube diameter. Water as working fluid attained an efficiency of 0.5 at 0.1 m tube diameter.

(a) Variation of efficiency with tube diameter (0.025 wt. %)

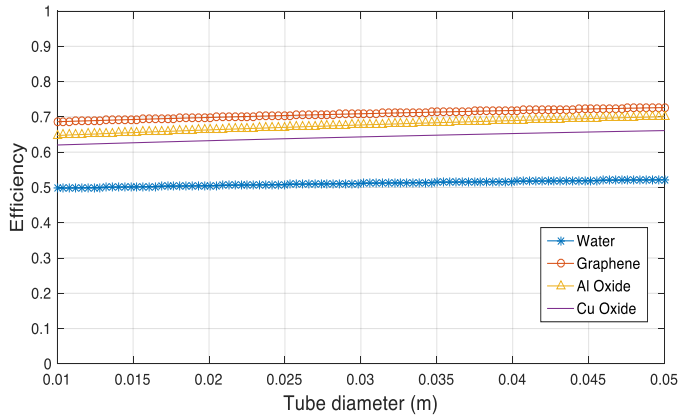

(b) Variation of efficiency with tube diameter (0.05 wt. %)

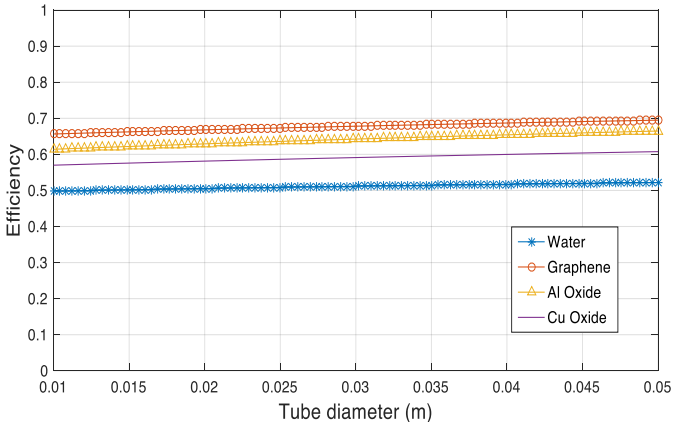

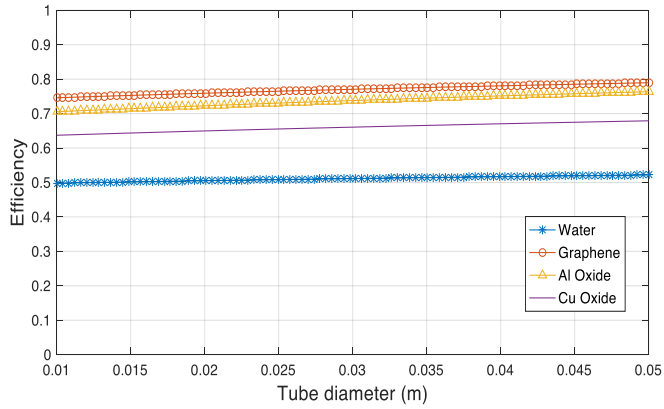

(c) Variation of efficiency with tube diameter (0.075 wt. %)

Fig. 5. Variation of efficiency with tube diameter

Figs. 6 (a) to 6 (c) show the variation of efficiency with reduced temperature parameter for all the working fluids at mass fractions of nano particles of 0.025, 0.05 and 0.075 wt. % respectively. It is observed from the figures that the efficiency increases as the reduced temperature parameter decreases. This is expected as the decrease in reduced temperature parameter implies decrease in losses, which leads to improved efficiency. Lines of each of the working fluids can be seen to intersect the efficiency axis at various points. At these points, $T_i = T_a$ and the efficiency of the collector is at its maximum value. These points are referred to as the zero loss efficiency point.

It can be seen from the figs. 6 (a) to 6 (c), that the collector efficiency at the zero loss efficiency points increases with increase in mass fraction of nano particles for each of the nano working fluids. This is because of the increased thermal conductivity which enhances convective heat transfer. Each of the nano working fluids produced maximum zero loss efficiency at 0.075 wt. %. Maximum efficiencies of 0.73, 0.7 and 0.68 were attained by graphene, aluminium oxide and copper oxide nano working fluids, while water attained efficiency of 0.56.

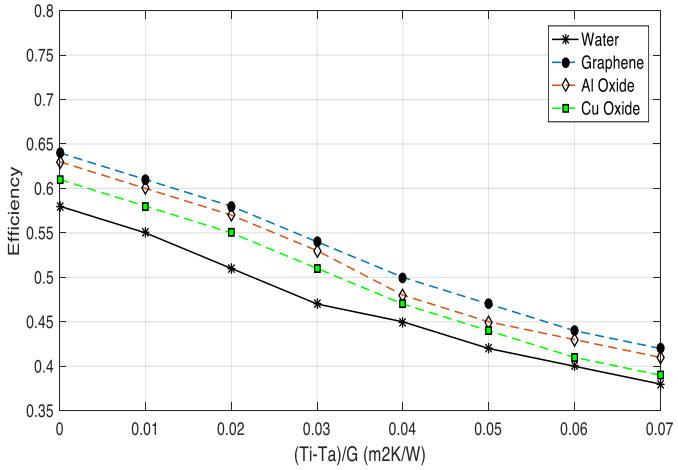

(a) Variation of efficiency with reduced temperature parameter (0.025 wt. %)

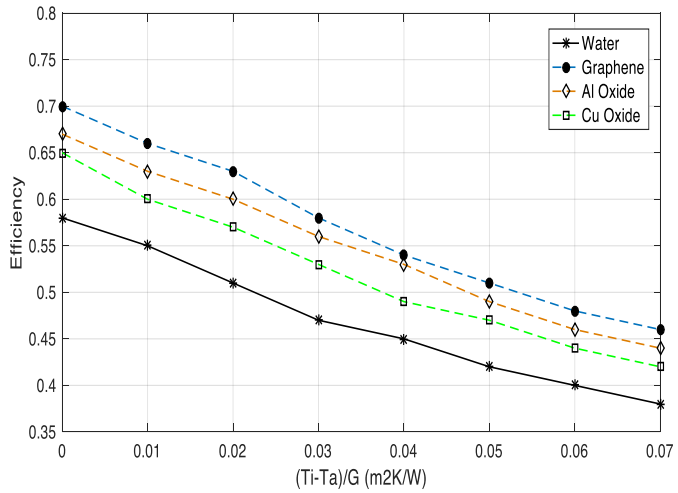

(b) Variation of efficiency with reduced temperature parameter (0.05 wt. %)

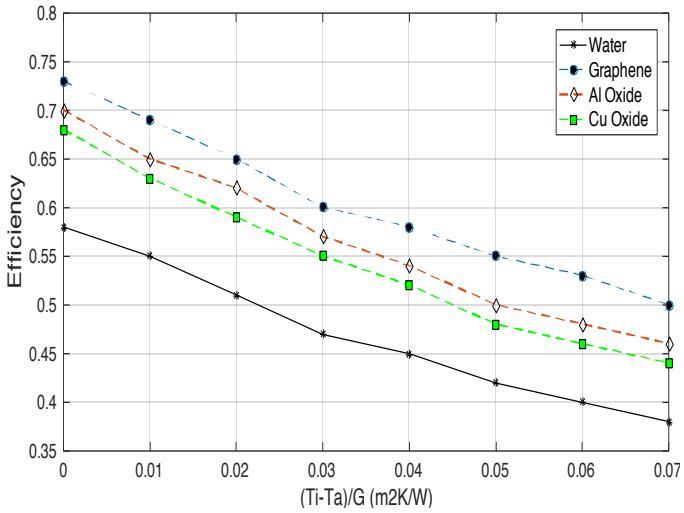

(c) Variation of efficiency with reduced temperature parameter (0.075 wt. %)

Fig. 6. Variation of efficiency with reduced temperature parameter

Fig. 7 shows the variation of zero loss efficiency with mass fraction for the nanofluids compared with zero loss efficiency for water. It can be observed that efficiency increases as mass fraction of nanofliuds increase. Water attained zero loss efficiency of 0.57. Maximum zero loss efficiencies of 0.73, 0.7 and 0.68 are seen for graphene, aluminium oxide and copper oxide respectively at 0.075 wt. %.These correspond to 28%, 22.8% and 19.2% increase respectively over the efficiency of water. Reference [13] reported increase in collector efficiency by 24.9% over base fluid (water) at 0.1 wt. % of graphene nanofluid. Reference [15] reported increase in efficiency by 18.8% over base fluid (water) at 0.025 wt. % of graphene nanofluid. From fig. 7, increase in efficiency of 0.025 wt. % graphene nanofluid over water can be observed to be 12.3%. Reference [12] reported increase in efficiency by 24% over base fluid (water) at 0.05 wt. % of Cu – water nanofluid. From fig. 7, increase in efficiency of 0.05 wt. % copper oxide nanofluid over water can be observed to be 14%.

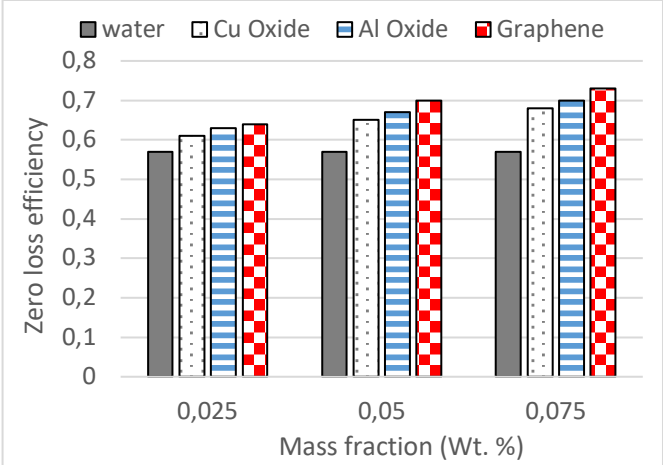

Fig. 7. Variation of zero loss efficiency with mass fraction

4.0 Conclusion

Flat plate solar collector efficiency has been simulated using water and three different nano working fluids. Collector performance equations were programmed and simulated in MATLAB. Tube spacing, mass flow rate and tube diameter were varied for each of the working fluids at nano particle mass fractions of 0.025, 0.05 and 0.075 wt. %. The effects of variation of parameters on collector efficiency were determined. Results indicate that the highest efficiencies were obtained at mass fraction of 0.075 wt. % for each of the nano working fluids. Graphene nano working fluid produced the highest collector efficiencies, followed by aluminium oxide nano working fluid and then copper oxide nano working fluid. Water as working fluid produced the least efficiencies. Increase in collector efficiency attained by the nano working fluids over water as working fluid were 28%, 22.8% and 19.2% for graphene, aluminium oxide and copper oxide nano working fluids respectively. The study has presented a method to size collector design parameters to obtain the values of the parameters that maximizes collector efficiency. Also, results obtained show that the nano

working fluids studied have potential to improve flat plate solar collector efficiency.

References

[1] G. Kumar, K. Sridhar and S. Kumar. "Heat removal factor of an integrated solar flat plate collector with packed bed system". International journal of engineering technology, management and applied sciences. 5 (7), 720 – 727, 2017.

[2] N. Sint, I. Choudhury, H. Masjuki and H. Aoyama. "Theoritical analysis to determine the efficiency of a CuO – water nanofluid based flat plate solar collector for domestic water heating system in Myanmar." Solar energy, 155, 608 – 619, 2017.

[3] M. Bhatt, S. Gaderia and S. Channiwala. "Experimental investigations on top loss coefficients of solar flat plate collector at different tilt angle." Journal of world academy of science engineering and technology. 79, 432 – 436, 2011.

[4] M. Mkhize and V. Msomi. "Feasibility of multistage solar still in southern Africa." In proceedings of 2020 9th international conference on renewable energy research and applications (ICRERA). 48 – 54. 2020.

[5] Y. Choi. "Performance improvement of liquid type solar heat collection system." In proceedings of 2018 7th international conference on renewable energy research and applications (ICRERA). 215 – 220. 2018.

[6] P. Ranjith and A. Aftab . "A comparative study on the experimental and computational analysis of solar flat plate collector using an alternative working fluid." Procedia technology, 24, 546 – 553, 2016.

[7] J. Wisam, G. Habib, T. Hassan and R. Hadi. "Enhanced heat transfer performance of a flat plate solar collector using CuO/ water and TiO/ water nanofluids." International journal of applied engineering research. 13 (6), 3673 – 3682, 2018.

[8] V. Msomi and O. Nemraoui. "Improvement of the performance of solar water heater based on nanotechnology." In proceedings of 2017 6th international conference on renewable energy research and applications (ICRERA). 524 – 527. 2017

[9] N. Akram, R. Sadri, S. Kazi, S. Ahmed, M. Zubir and M. Ridha. "An experimental investigation on the performance of a flat plate solar collector using eco – friendly treated graphene nanoplatetets – water nanofluids." Journal of thermal analysis and calorimetry, 138 (1), 609 – 621, 2019

[10] Y. Lee, J. Hyomin, P. Ji – tae, D. Antonio and K. Sedong. "Experimental investigation on evaluation of thermal performance of solar heating systems using Al_2O_3 nanofluid." Applied sciences. 1 – 9, 2020.

[11] O. Alawi, H. Kamar, A. Mallah, H. Mohammed, M. Sabrudin, K. Newaz, G. Najafi and Z. Yaseen. "Experimental and theoretical analysis of energy efficiency in flat plate solar collector using monolayer graphene nanofluids." Sustainability, 1 – 22, 2021.

[12] M. Jamal – Abad, A. Zamzamian, E. Imani and M. Mansouri. "Experimental study of the performance of a flat plate solar collector using Cu – water nanofluid." Journal of thermophysics and heat transfer, 27(4): 756 – 760, 2013.

[13] L. Kumar, S. Kazi, H. Masjuki, M. Zubir, A. Jahan and C. Bhinitha. "Energy, exergy and economic analysis of liquid flat plate solar collector using green covalent functionalized graphene nanoplatelets." Applied thermal engineering, 192, 1 – 19. 2021.

[14] H. Huang, T. Coote, N. Bristow, T. David, J. Kettle and G. Todeschini. "Development of an improved computer model for organic photovoltaic cells." In proceedings of 2020 9th international conference on renewable energy research and applications (ICRERA). 78 – 82. 2020.

[15] A. Ahmadi, D. Ganji and F. Jafarkazemi. "Analysis of utilizing graphene nanoplatelets to enhance thermal performance of flat plate solar collectors." Energy conversion and management, 126: 1 – 11, 2016.

[16] K. Elsaid, M, Abdelkareem, H. Maghrabie, E. Sayed, T. Wilberforce A. Baroutaji and A. Olabi. "Thermo physical properties of graphene based nano fluids." International journal of thermo fluids10: 1 – 12, 2021.

[17] U. Uyor, P. Popoola and O. Popoola. "Improved energy storage performance of insulated graphene/ polymer nanocomposites." In proceedings of 2018 7th international conference on renewable energy research and applications (ICRERA). 189 – 193. 2018.

[18] T. Tun – Ping, and H. Yi – Hsuan. "Estimation and experimental study of the density and specific heat for alumina nanofluid." Journal of experimental nanoscience. 9(7), 1 – 13, 2014.

[19] R. Mondragon, D. Sanchez, R. Cabello, R. Liopis and J. Julia. "Flat plate solar collector performance using alumina nanofluids: Experimental characterization and efficiency tests." PLoS ONE 14(2): e0212260. https://doi.org/ 10.1371/journal.pone.0212260, 2019.

[20] T. Kitano, T. Kataoka and T. Shirota. "An empirical equation of relative viscosity of polymer melts filled with various inorganic fillers." Rheologica Act. 20(2): 207 – 209, 1981.

[21] J. Duffie and W. Beckman. Solar engineering of thermal processes. 4th Edition John Wiley and Sons Inc.,

111 River Street Hoboken, New Jersey, U.S.A. 2013. pp. 236 – 667.

[22] L. Theodore S. Adrienne P. Frank and P. David. Fundamentals of heat and mass transfer. 7th edition, John Wiley and sons. Ltd. 2011.

Nomenclature

A_c: Area of collector (m^2)
B: Collector width (m)
C_b: Bond conductance
C_p: Fluid specific heat capacity (J/kgC)
D_i: Tube inner diameter (m)
D_o: Tube outer diameter (m)
f: Friction factor
F: Standard fin efficiency
F': Collector efficiency factor
F_R: Heat removal factor
G: Solar radiation (W/m^2)
h_{fi}: Fluid to tube heat transfer coefficient (W/m^2C)
h_w: Wind heat transfer coefficient (W/m^2C)
H: Collector height (m)
k: Thermal conductivity (W/mC)
k_i: Insulation thermal conductivity (W/mC)
l_i: Insulation thickness (W/mC)
L: Collector length (m)
$\dot{m}$: Fluid mass flow rate (kg/s)
N: Number of glass covers
Pr: Prandtl number
Q_u: Useful energy gain (W)
Re: Reynolds number
T_{amb}: Ambient temperature (C)
T_i: Fluid inlet temperature (C)
T_o: Fluid outlet temperature (C)
T_{pm}: Mean plate temperature *(C)*
U_b: Back heat loss coefficient (W/m^2C)
U_e: Edge heat loss coefficient (W/m^2C)
U_t: Top heat loss coefficient (W/m^2C)
U_L: Overall heat loss coefficient (W/m^2C)
v: Velocity (m/s)
W: Tube spacing (m)

Greek

β: Collector tilt angle
ε_g: Emittance of glass
ε_p: Emittance of plate
σ: Boltzman constant (W/m^{2}K)
ω: Mass concentration (kg)
ρ: Fluid density (kg/m^3)
μ: Dynamic viscosity (kg/m.s)
δ: Plate thickness (m)
η: Efficiency

Subscript

nf: Nano fluid
np: Nano particle
bf: Base fluid
p: Plate

Acronym

MATLAB: Matrix laboratory
TRNSYS: Transient Systems Simulation software